Mechanisms of Spontaneous Two-Electron Emission from Core-Excited States of Molecular CO

T. Kaneyasu,[1,*] Y. Hikosaka,[1] P. Lablanquie,[2,3] F. Penent,[2,3] L. Andric,[2,3] G. Gamblin,[2,3] J. H. D. Eland,[4] Y. Tamenori,[5] T. Matsushita,[5] and E. Shigemasa[1]

[1]*UVSOR Facility, Institute for Molecular Science, Okazaki 444-8585, Japan*
[2]*UPMC Université Paris 06, LCPMR, 11 rue Pierre et Marie Curie, 75231 Paris Cedex 05, France*
[3]*CNRS, LCPMR (UMR 7614), 75231 Paris Cedex 05, France*
[4]*Physical and Theoretical Chemistry Laboratory, Oxford OX1 3QZ, United Kingdom*
[5]*Japan Synchrotron Radiation Research Institue, Sayo, Hyogo 679-5198, Japan*

(Received 13 April 2008; published 29 October 2008)

We demonstrate that the observation of slow electrons emitted in the decay of molecular core-excited states can be a sensitive probe of the double Auger processes, and that in combination with electron-electron coincidence spectroscopy, it can provide clear insight into the mechanisms involved. The present study identifies all cascade Auger paths from the C1*s*-to-Rydberg states in CO to final states of CO^{2+}. One pathway includes the first directly identified case of molecular level-to-level autoionization of a cation and shows remarkable selectivity for a specific final state.

DOI: 10.1103/PhysRevLett.101.183003 PACS numbers: 32.80.Hd, 33.20.Tp, 33.80.Eh, 33.80.Gj

Neutral core-excited states of low-Z atoms relax mainly by electron emission (''resonant Auger decay''), which has been investigated intensively in rare gases [1]. It leads predominantly to singly charged ions, but formation of doubly charged ions by emission of two Auger electrons (''resonant double Auger decay'') also makes up a considerable fraction of the total decay [2,3]. In resonant double Auger decay, one of the two electrons is often slow, with a kinetic energy typically less than 10 eV. Understanding of the formation mechanism of such slow electrons is particularly relevant in radiation biology [4,5] and surface photochemistry [6], because low energy electron collisions play crucial roles in the chemical reactions involved there.

Both direct and indirect processes can contribute to resonant double Auger decay [7]. In the direct process (also called Auger shake-off), which is entirely due to the electron correlation, two electrons are simultaneously ejected and the available energy is continuously shared between the two electrons. In the indirect process (cascade Auger decay), two electrons are emitted sequentially with distinct kinetic energies depending on the energy levels of the initial, intermediate, and final electronic states involved. Since the recent successful introduction of a new multidimensional electron spectroscopy by Eland *et al.* [8], the important role of indirect processes for producing low energy electrons in the decay processes of core-hole states is being revealed. The usefulness of detecting such slow electrons has been clearly demonstrated in recent high-resolution electron spectroscopic studies of rare gases ([9] and references therein).

Resonant double Auger decay of molecules must be expected to occur by analogy with this established process in atoms and is indeed known to exist from mass spectroscopic studies of ions [10,11]. However, the molecular process is much more complicated than the atomic one because it can be influenced by nuclear motions at any stage of the decay. For example, singly charged molecular ion states populated by the first electron emission can undergo competition between second electron emission and molecular dissociation. If one of the dissociating fragments is excited, it may subsequently autoionize. By analogy with the atomic process, molecular autoionization from intermediate superexcited cation states to molecular dication states should exist; this process has often been postulated, but has never been clearly observed directly.

In this Letter, we demonstrate that observation of slow electrons emitted in the decay of molecular core-excited states can be a sensitive probe of the double Auger processes and that the mechanisms of the complicated molecular double Auger decay can be clarified by the combined use of high-resolution electron spectroscopy and electron-electron coincidence spectroscopy. We have used two different experimental setups. High-resolution electron spectroscopy using a hemispherical electron analyzer (Gammadata-Scienta SES-2002) was performed at beam line 27SU [12] of SPring-8. Linearly polarized light from a figure-8 undulator was monochromatized by a grazing incidence monochromator and focused into a gas cell. Electrons emitted parallel to the electric vector were analyzed. The second experiment, electron-electron coincidence spectroscopy, was carried out at the beam line UE56/2-PGM1 [13] of BESSY II with a magnetic-bottle electron spectrometer [8,14,15]. The storage ring was operated in single-bunch mode, which provides 800.5 ns periodic light pulses. Electrons were analyzed in energy by their time of flight in the magnetic-bottle electron spectrometer. The energy resolution of the spectrometer was estimated to be $\Delta E/E \sim 1.5\%$ (limited to $\Delta E \sim$ 10 meV below 0.5 eV).

Figure 1 shows a two-dimensional (2D) map of slow electron yields as a function of the photon energy in the C1*s* Rydberg excitation region of CO, with the total ion

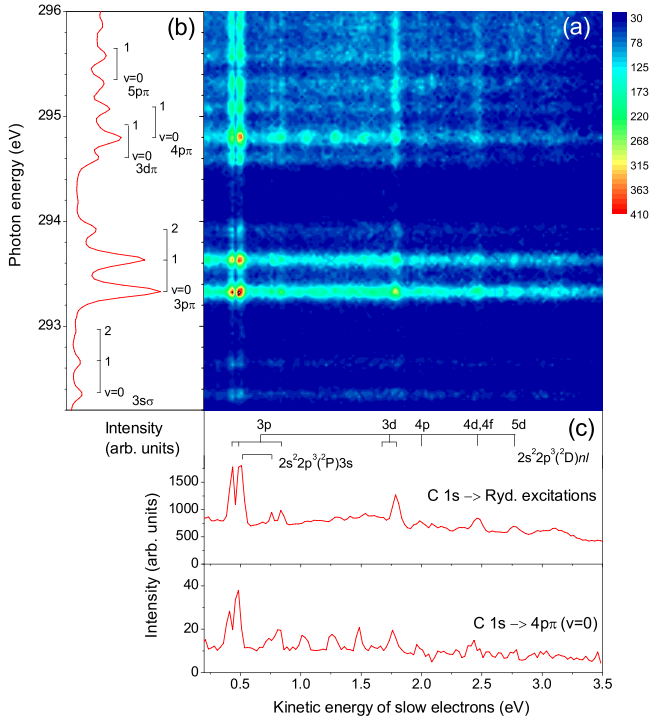

FIG. 1 (color online). (a) Two-dimensional (2D) map of the slow electron yields in the C1s-to-Rydberg range. The yields are obtained in a 30 meV photon energy step and in a 25 meV kinetic energy step. The energy resolution of the analyzer was set to 63 meV, and the photon energy resolution to 100 meV. (b) Total ion yield spectrum. (c) Top: Sum of the slow electron yields in the Rydberg excitation region which is derived by projecting the electron yields in the 2D map onto the horizontal axis. Bottom: Slow electron spectrum at the C1$s \rightarrow 4p\pi(v = 0)$ resonance.

yield spectrum measured together with the slow electron yields. The 2D map exhibits horizontal stripes in the Rydberg resonances. Such slow electrons can be produced only by double (or multiple) Auger decay, and high discrimination against the dominant single Auger decay is achieved by setting the observation window to these low energy electrons. While direct double Auger emissions result in a continuous energy electron energy distribution, sequential processes can produce discrete structures in the energy distribution. In practice, knots of enhancement are discernible in each stripe on the 2D map. The locations of some of these knots are common to all different C1s-to-Rydberg excitations. In order to closely inspect these discrete structures, the slow electron yields on the 2D map are projected onto the horizontal axis. Most of the peaks observed in the resultant spectrum [Fig. 1(c)] can be assigned to autoionization of highly excited atomic oxygen states into the ionic ground state $O^+(^4S)$ [16–18]. This observation implies that dissociation of CO^+ states formed by first-step Auger decay and subsequent fragment O^* atom autoionization constitute a major path for the double Auger decay of the C1s-to-Rydberg states. Such processes where nuclear motion precedes electron emission have been noted before [19]; their prevalence is quite surprising and is still not fully understood.

In the 2D map (Fig. 1), we also find additional spots appearing only on the $4p\pi(v = 0)$ resonance. These spots are spaced at 0.24 eV intervals, as clearly seen in the horizontal cut of the 2D map on this resonance [bottom panel of Fig. 1(c)]. The constant intervals suggest that the peaks correspond to vibrational levels of CO^+ or CO^{2+}, and are therefore associated with molecular autoionization of CO^+ into CO^{2+}. Here, a question arises: why is the molecular process enhanced only in the double Auger decay of the $4p\pi(v = 0)$ state? In order to identify the relevant resonant Auger process more exactly, we have performed electron-electron coincidence measurements by tuning the photon energy to the $4p\pi(v = 0)$ resonance. Figure 2(a) shows kinetic energy correlations between the two electrons ejected at this photon energy. The vertical and horizontal axes of the energy correlation map correspond to the kinetic energies of the fast and slow Auger electrons, respectively. Here, the experimental resolutions for the fast and slow electrons are of the order of 4 eV and

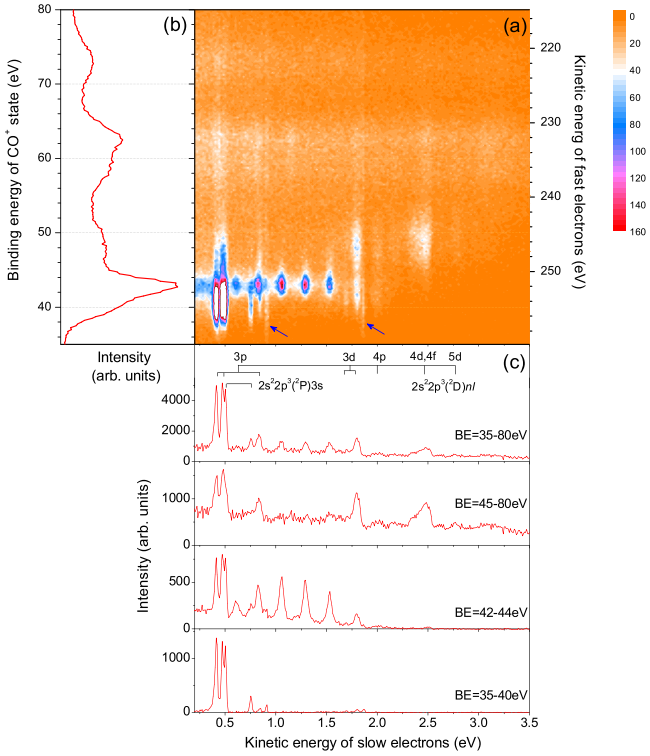

FIG. 2 (color online). (a) Correlation map for kinetic energies of electron coincidence pairs emitted at the $4p\pi(v = 0)$ resonance. The coincidence data set is obtained at $h\nu = 294.8$ eV with the photon energy resolution of 100 meV. Note that weak vertical lines denoted by arrows are due to false coincidences. (b) Resonant Auger spectrum on a CO^+ binding energy scale, obtained by integrating the coincidence yields. The spectrum shows only the resonant Auger structures relevant to slow electron emission. (c) Slow electron spectra integrated for selected binding energy ranges indicated on the correlation map.

20 meV, respectively. The fast Auger electron spectrum in Fig. 2(b), obtained by projecting the coincidence map onto the vertical axis, shows the CO^+ states involved in the double Auger process. In this binding energy range, the CO^+ states are populated by "spectator" Auger decay, in which the initially excited Rydberg electron remains passive, but not necessarily unmoved.

The energy correlation map reveals that the molecular autoionization peaks are related to a state of CO^+ lying around a binding energy of 43 eV. In addition, the formation of O^* fragments is discernible at particular binding energies and background is enhanced around the CO^+ states lying above 55 eV. Direct double Auger decay should appear as diagonal structures on the energy correlation map because the sum of kinetic energies of the two Auger electrons is constant according to the formation of individual final CO^{2+} states. Diagonal structures due to the direct double Auger processes are, however, hardly recognizable in Fig. 2, which indicates that the double Auger decay of the $4p\pi$ state is dominated by cascade processes. The same propensity is observed in double Auger decay of the $C1s \rightarrow \pi^*$ state [20] and also of other $C1s$-to-Rydberg states [21].

For a clear display of evolution of the second-step Auger decay with relevant CO^+ states, coincidence yields integrated in selected binding energy regions are plotted in Fig. 2(c). Strong peaks due to atomic oxygen autoionization are observed in the spectrum in the binding energy range 35–40 eV, which is below the adiabatic double ionization threshold (41.325 eV [22]) of CO. The formation of the O^* fragments in the 35–40 eV binding energy range is attributable to predissociation of CO^+ states lying below $CO^{2+}(X^3\Pi)$ into repulsive states correlating to $C^+ + O^*$ limits, which is already known in valence double photoionization [23]. The same CO^+ states can hence be produced via the first-step Auger decay from the $4p\pi(v = 0)$ resonance.

In the 45–55 eV binding energy range, autoionization lines associated with formation of the O^* fragments with $n = 3$–4 are dominantly observed [see Fig. 2(a)]. The formation of the $O^*[O^+(^2D)4d/4f]$ fragments is particularly enhanced, as compared to the lower binding energy range. This enhancement can be understood if the principal quantum numbers of the precursor CO^+ states populated by spectator Auger decay are $n \sim 4$, and this principal quantum number is conserved during the dissociation producing the O^* fragments. In the binding energy region above 55 eV, an enhanced background is definitively observed together with weak atomic oxygen lines. Molecular autoionization from the CO^+ states lying in this binding energy range can populate numerous CO^{2+} states with repulsive potential energy curves; the background enhancements can be understood as due to such autoionization of CO^+.

The energy resolution of electron-electron coincidence spectroscopy is not sufficient to clearly identify the CO^+ state relevant to the molecular autoionization seen around the binding energy of 43 eV. On the other hand, conventional electron spectroscopy can locate such CO^+ states with high resolution. Figure 3(a) shows a high-resolution resonant Auger spectrum at the photon energy corresponding to the $4p\pi(v = 0)$ resonance. The spectrum exhibits a strong peak at a binding energy of 43.05 eV; because of the close agreement in binding energy, the peak can be identified with the CO^+ level relevant to the molecular autoionization. The peak width is around 100 meV, which corresponds exactly to the experimental resolution. It seems probable that the natural width of the CO^+ state at 43.05 eV is less than 50 meV, taking into account the errors in estimating the experimental resolution. This CO^+ state is assigned as the $v = 0$ level of a Rydberg-type CO^+ state $[CO^{2+}(d^1\Sigma) + 5p]$ whose population comes from Auger shake-up behavior of the Rydberg electron [24]. The minimum of the inner well on the potential curve of the Rydberg-type CO^+ state lies close to the equilibrium nuclear distance of the $CO^+(1s^{-1})$ state, and the same situation can reasonably be assumed for $CO(1s^{-1}4p\pi)$; thus, only the vibrational ground level of the CO^+ intermediate state is noticeably populated from the initial $4p\pi(v = 0)$ resonance [25]. By the same argument, the $(v = 1)$ level should be populated from the $(v = 1)$ resonance.

The potential energy curve of the Rydberg-type CO^+ state is depicted in Fig. 3(b), as well as the calculated curves of CO^{2+} states [26]. Here, we assume that the potential energy curve of the Rydberg-type CO^+ state is parallel to that of the $CO^{2+}(d^1\Sigma)$ state [27]. This CO^+ state is energetically allowed to autoionize into the low-lying three bound $X^3\Pi$, $a^1\Sigma$, and $b^1\Pi$ states of CO^{2+}. The calculated FC factors for the autoionization into these CO^{2+} states are plotted in Fig. 4, for comparison with the slow electron spectrum associated with the CO^+ state in the binding energy range of 42–44 eV. The FC factors were calculated by assuming Morse potentials for the relevant CO^+ and CO^{2+} states, where the spectroscopic

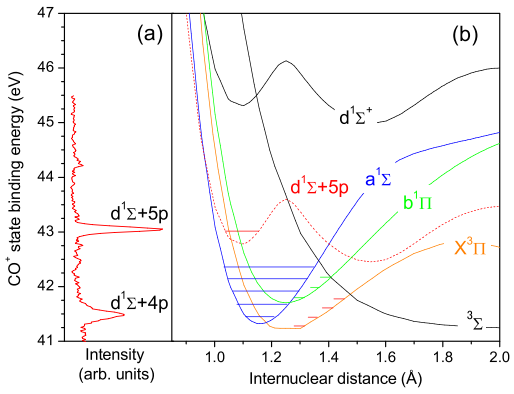

FIG. 3 (color online). (a) High-resolution resonant Auger spectrum measured at the $4p\pi(v = 0)$ resonance. The energy resolution of the analyzer was set to 78 meV, and the photon energy resolution to 60 meV. (b) Potential energy curves of the Rydberg-type $CO^+[CO^{2+}(d^1\Sigma) + 5p]$ (dotted line) and CO^{2+} states (solid lines).

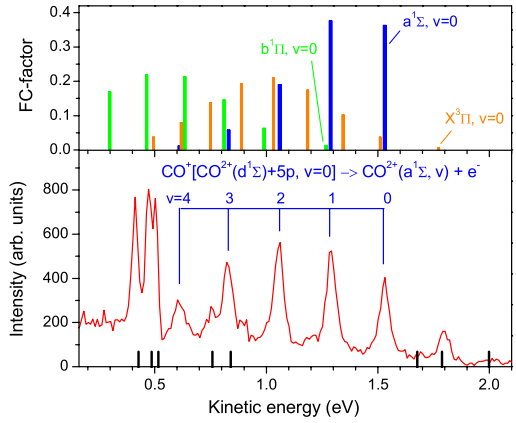

FIG. 4 (color online). Bottom: Second-step electron spectrum derived from the correlation map in Fig. 2, which is associated with fast electrons corresponding to the binding energy region between 42 and 44 eV. The vertical bars in the spectrum indicate autoionization lines of O* fragments. Top: Calculated Franck-Condon factors for different final states.

constants determined by Püttner *et al* [28] are used. Note that, although the general shapes of the potential energy curves are far from pure Morse potential form, the vibrational distributions of the CO^{2+} states in the C1s normal Auger spectrum are reasonably reproduced [28]. One can see in Fig. 4 that the molecular autoionization peaks in the slow electron spectrum are unambiguously assigned to the autoionization into the $v = 0$–4 levels of the $CO^{2+}(a^1\Sigma)$ state. The fit confirms this first direct observation of level-to-level autoionization in a cation. The populations of higher vibrational levels are enhanced relative to those in the FC analysis, which may be attributable to insufficient accuracy of the potential energy curve assumed for the CO^+ state. Alternatively, autoionization from the outer well range, which can be accessed by tunneling, might populate high vibrational levels. In contrast, peaks corresponding to the autoionization into the other two CO^{2+} states are hardly detectable in the slow electron spectrum in Fig. 4. The autoionization of this Rydberg-type CO^+ state populates the final $CO^{2+}(a^1\Sigma)$ state with strong specificity, for which no reason can yet be given. The lack of any similar process associated with the ($v = 1$) resonance is also surprising, but might possibly be explained if the intermediate state decays rapidly by a tunneling process.

In the decay of the C1$s \rightarrow 4p\pi(v = 0)$ state, level-to-level molecular autoionization from CO^+ into CO^{2+} showing a remarkable electronic specificity has been unambiguously revealed. To our knowledge, this is the first directly identified case of molecular level-to-level autoionization of a cation. The spectra show that other CO^+ intermediate states populated by the first-step Auger decay dissociate into fragment pairs $C^+ + O^*$ instead of autoionizing in the molecular range. This is the common fate of superexcited states of many small molecular ions, formed at photon energies below inner shell thresholds [29]. The reason for the exceptional behavior of the CO^+ [$CO^{2+}(d^1\Sigma) + 5p$, $v = 0$] level is not yet understood, but may be connected with its stability.

We thank M. Simon, R. Guillemin, and L. Journel (LCPMR) for their scientific impetus and many fruitful discussions on the present study, and A. Hishikawa (IMS) for his help on the FC analysis. J. H. D. E. thanks the Leverhulme Trust for support. The experiment of high-resolution electron spectroscopy was carried out with the approval of the JASRI (No. 2006A1516). This work has been supported by Grant-in-Aid for Scientific Research from the JSPS, and in part by the European Community, Research Infrastructure Action under the FP6 "Structuring European research Area" Programme (contract R II 3-CT-2004-506008).

*Present address: Kyushu Synchrotron Light Research Center, Saga 841-0005, Japan.

[1] G. B. Armen *et al.*, J. Phys. B **33**, R49 (2000).
[2] J. Viefhaus *et al.*, Phys. Rev. Lett. **92**, 083001 (2004).
[3] J. Viefhaus *et al.*, J. Electron Spectrosc. Relat. Phenom. **141**, 121 (2004).
[4] B. Boudaiffa *et al.*, Science **287**, 1658 (2000).
[5] C. König, J. Kopyra, I. Bald, and E. Illenberger, Phys. Rev. Lett. **97**, 018105 (2006).
[6] R. Balog and E. Illenberger, Phys. Rev. Lett. **91**, 213201 (2003).
[7] J. Viefhaus *et al.*, J. Phys. B **38**, 3885 (2005).
[8] J. H. D. Eland *et al.*, Phys. Rev. Lett. **90**, 053003 (2003).
[9] S.-M. Huttula *et al.*, Phys. Rev. A **67**, 052703 (2003).
[10] A. P. Hitchcock *et al.*, Phys. Rev. A **37**, 2448 (1988).
[11] N. Saito *et al.*, Phys. Rev. A **51**, R4313 (1995).
[12] H. Ohashi *et al.*, Nucl. Instrum. Methods Phys. Res., Sect. A **467–468**, 533 (2001).
[13] K. J. S. Sawney *et al.*, Nucl. Instrum. Methods Phys. Res., Sect. A **390**, 395 (1997).
[14] F. Penent *et al.*, Phys. Rev. Lett. **95**, 083002 (2005).
[15] P. Lablanquie *et al.*, J. Electron Spectrosc. Relat. Phenom. **156–158**, 51 (2007).
[16] V. Čermák and J. Šrámek, J. Electron Spectrosc. Relat. Phenom. **2**, 97 (1973).
[17] F. Penent *et al.*, J. Phys. B **20**, 6065 (1987).
[18] A. A. Wills, A. A. Cafolla, and J. Comer, J. Phys. B **24**, 3989 (1991).
[19] E. Shigemasa *et al.*, J. Electron Spectrosc. Relat. Phenom. **156–158**, 289 (2007).
[20] L. Journel *et al.*, Phys. Rev. A **77**, 042710 (2008).
[21] T. Kaneyasu *et al.* (to be published).
[22] M. Hochlaf *et al.*, Chem. Phys. **207**, 159 (1996).
[23] Y. Hikosaka and J. H. D. Eland, Chem. Phys. **299**, 147 (2004).
[24] S. Sundin *et al.*, J. Phys. B **30**, 4267 (1997).
[25] S. Sundin *et al.*, Phys. Rev. A **56**, 480 (1997).
[26] J. H. D. Eland *et al.*, J. Phys. B **37**, 3197 (2004).
[27] N. Vinci and J. Tennyson, J. Phys. B **37**, 2011 (2004).
[28] R. Püttner *et al.*, Chem. Phys. Lett. **445**, 6 (2007).
[29] J. H. D. Eland, in Advances in Chemical Physics 2008 (to be published).